

## Supporting Information

### Extracellular Matrix-Mimicking Magnetic Microrobot for Targeted Elimination of Circulating Cancer Cells

Jing Huang<sup>a,b†</sup>, Yuan Liu<sup>b†</sup>, Jiandong Wu<sup>b</sup>, Fuping Dong<sup>a\*</sup>, Chu Liu<sup>b</sup>, Jiawei Luo<sup>b</sup>, Xiangchao Liu<sup>b</sup>, Ning Wang<sup>b</sup>, Lei Wang<sup>b</sup>, Haifeng Xu<sup>b\*</sup>

<sup>a</sup> Department of Polymer Materials and Engineering, College of Materials and Metallurgy, Guizhou University, Guiyang, 550025, China

<sup>b</sup> Shenzhen Institute of Advanced Technology, Chinese Academy of Science, Shenzhen, Guangdong Province, P. R. China, 1068 Xueyuan Avenue, 518055 Shenzhen, China

#### Supplementary Figures

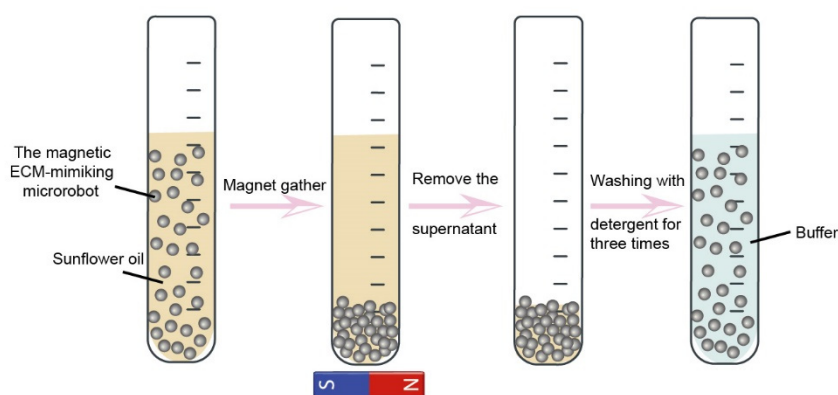


**Figure S1. Microrobots purification.** First, the prepared magnetic ECM-mimicking microrobots were dispersed in sunflower oil. Then the microrobots were gathered at the bottom of the centrifuge tube with a magnet, and the supernatant is removed at the same time. Finally, an appropriate amount of washing solution is added to the container to wash to microrobots for three times.

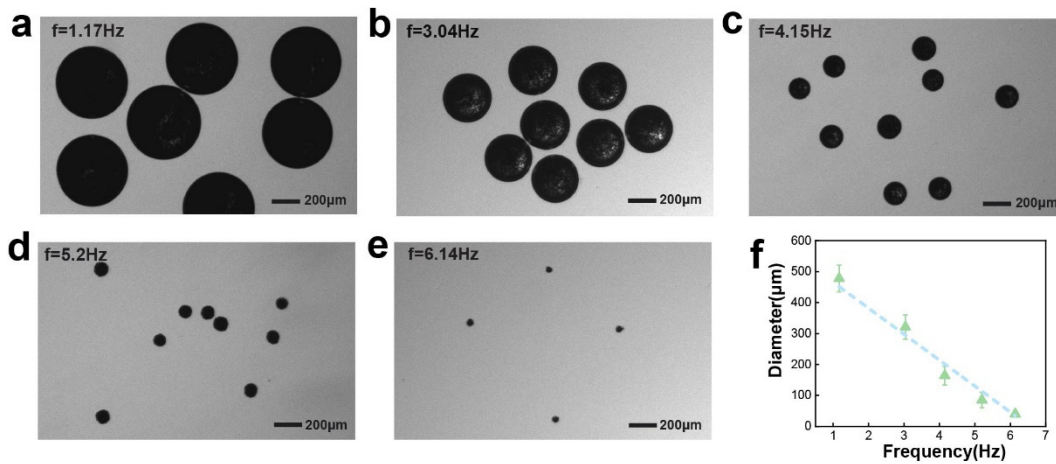


**Figure S2. Microrobot production.** (a)-(e) the diameter of the magnetic ECM-mimicking microrobot ranges from 30  $\mu\text{m}$  to 500  $\mu\text{m}$ , corresponding to the needle plunging frequency dropping from 6 Hz to 1 Hz. (f) The diameter of the magnetic ECM-mimicking microrobot is linearly related to the needle plunging frequency ( $r = 0.96$ ).

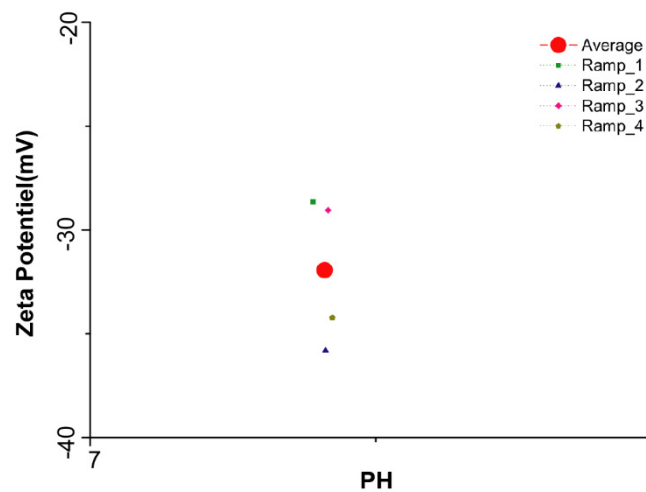


**Figure S3. Zeta potential of the magnetic ECM-mimicking microrobot.** The magnetic ECM-mimicking microrobot presented in this paper has a  $-32$  mV zeta potential at  $\text{PH}=7.4$ , indicating high stability and safety for applications in the blood.

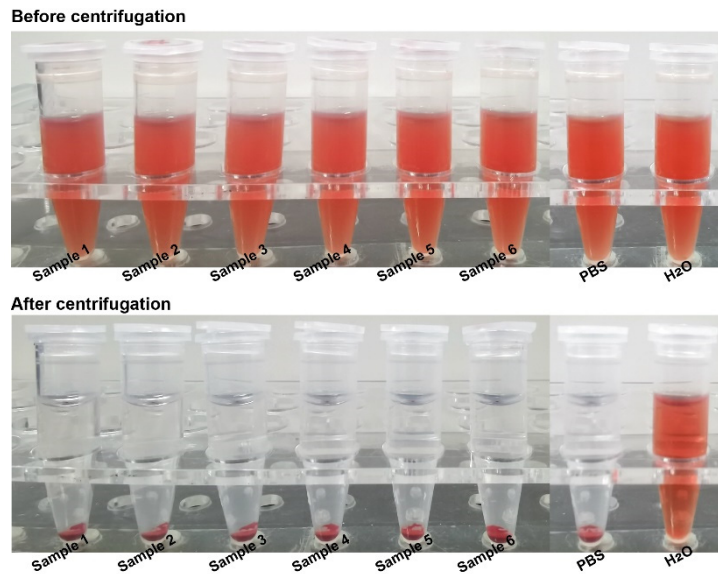


**Figure S4. Hemolysis test of microrobots.** Photograph of human red blood cells added with distilled water (positive control), normal saline (negative control), and microrobots. Hemolysis degree of tested microrobots for three hours. Hemolysis rate (%) =  $\frac{(\text{absorbance}(\text{test}) - \text{absorbance}(\text{negative control}))}{(\text{absorbance}(\text{positive control}) - \text{absorbance}(\text{negative control}))} \times 100\%$ . The light absorbance at 541 nm was measured. The hemolysis rate of the microrobot was  $0.46 \pm 0.42\%$ ,  $n=6$  samples, mean  $\pm$  sd.

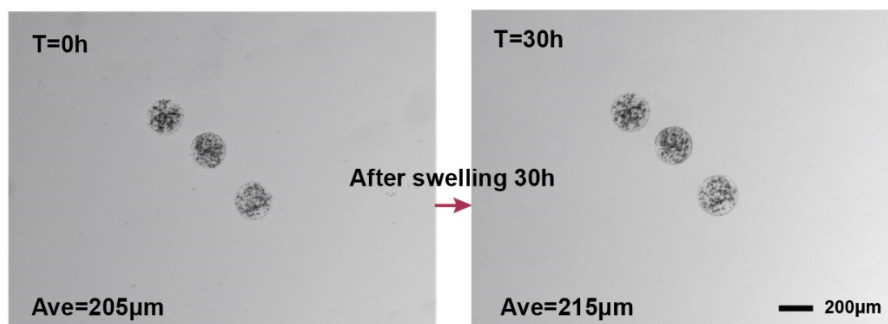


**Figure S5. Microrobot stability over time.** The microscope images of the magnetic ECM-mimicking microrobots swelled in the cancer cell culture buffer for 30h. It can be observed that the microrobots can stably retain their spherical shape, and the diameter of the microrobots is almost stable.

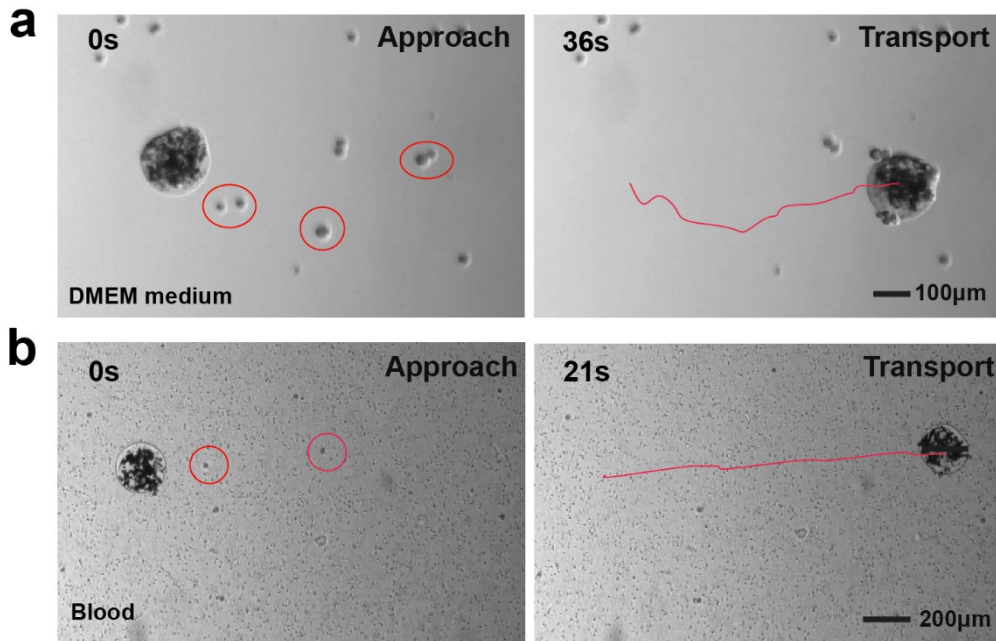


**Figure S6. Sensitivity test of the microrobot to capture circulating cancer cells.** (a) The magnetic ECM-mimicking microrobot captures the cancer cells located in the moving path in the DMEM medium. (b) The magnetic ECM-mimicking microrobot captures the cancer cells located in the moving path in the blood. The red line indicates the microrobot's trajectory.

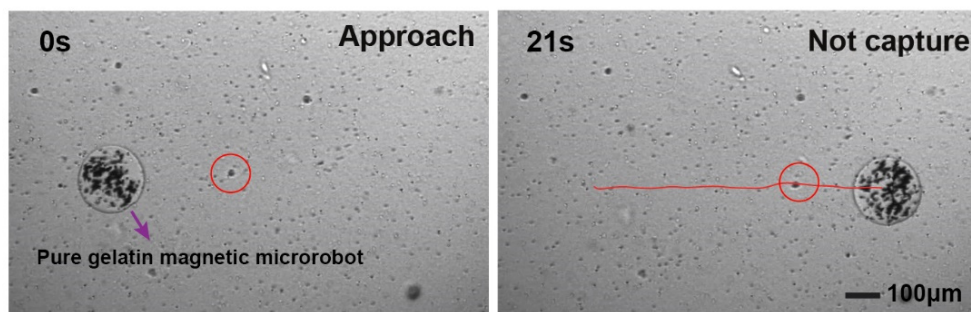


**Figure S7. Pure gelatin magnetic microrobot cannot capture cancer cells when pass by the cancer cell's surface.** The red line indicates the microrobot's trajectory.

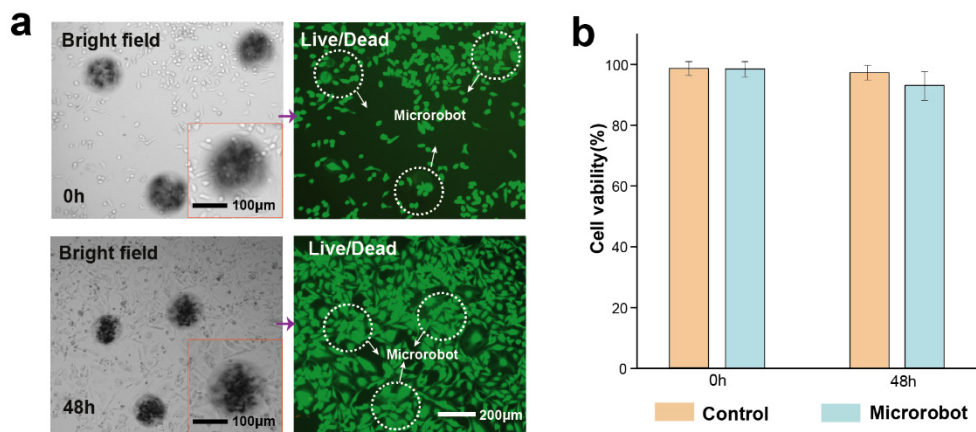


**Figure S8. Cytotoxicity test of the microrobot.** (A) Bright-field images and fluorescence images of 0-hour culture and 48-hour culture of cells with the microrobot. Live cells are indicated by the green fluorescence and dead cells are revealed by the red fluorescence. (B) MDA-MB-231 cells viability test by incubating with the magnetic ECM-mimicking microrobot for 48 h. ns =  $p > 0.05$  ( $n = 6$ ).

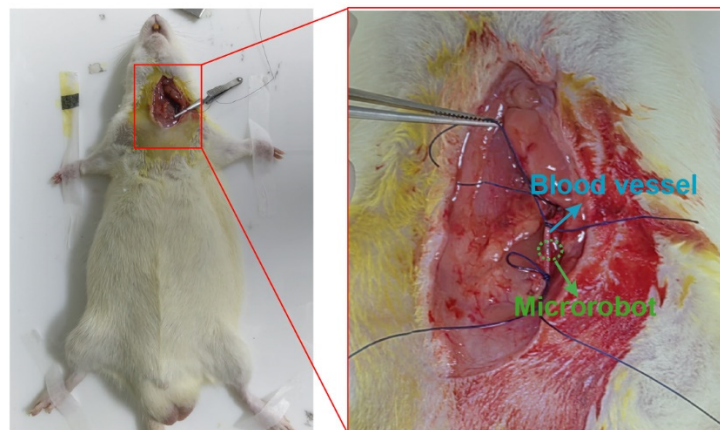


**Figure S9. In vivo application evaluation of the magnetic ECM-mimicking microrobot.** The proximal and distal ends of the peripheral venous vessels of the rat were ligated, leaving about 1 cm of blood vessels. Then the magnetic ECM-mimicking microrobot was implanted in the jugular vein of the rat.

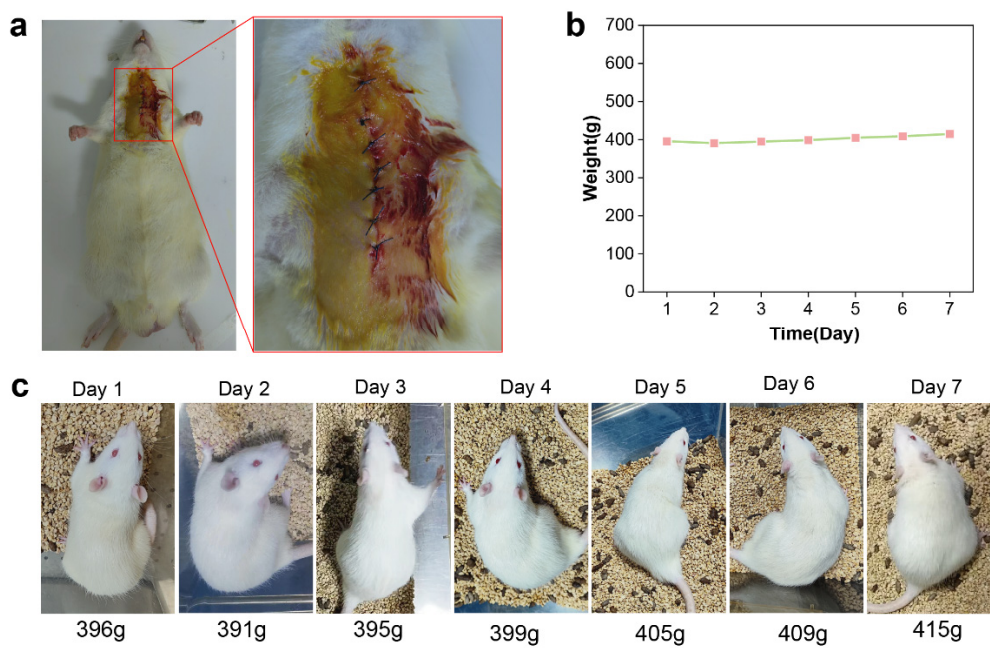


**Figure S10. Safety Assessment of the magnetic ECM-mimicking microrobot.** (a) Suturing and disinfecting wounds of the rat. (b) Weight records of the rat during the pathological analysis within 7 days. (c) Photographs of 7-day pathological analysis of the rat.

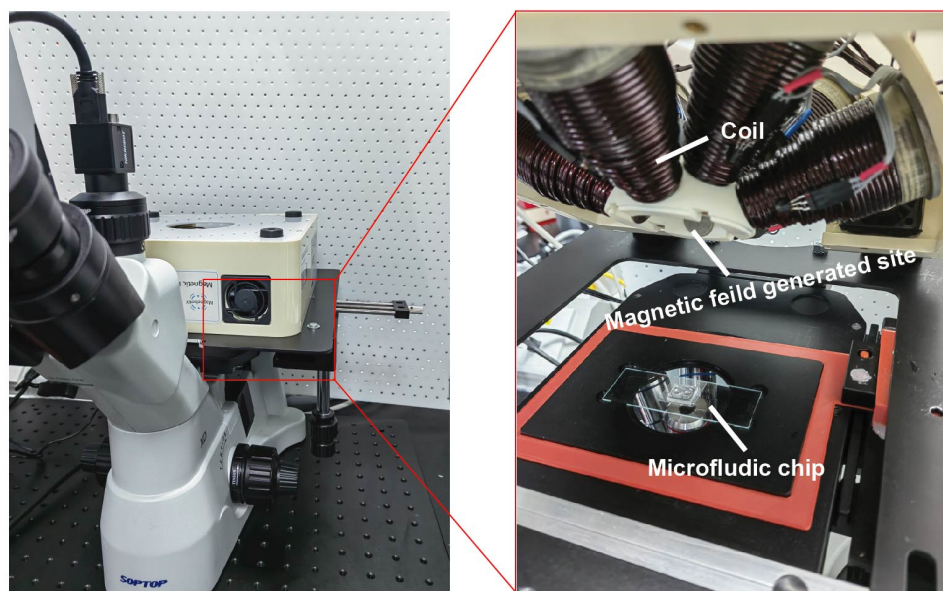


**Figure S11. Magnetic control system.** The microfluidic chip containing the buffer and the microrobot is located in the central part of the device. The eight magnetic coils that provide the controlled magnetic field.

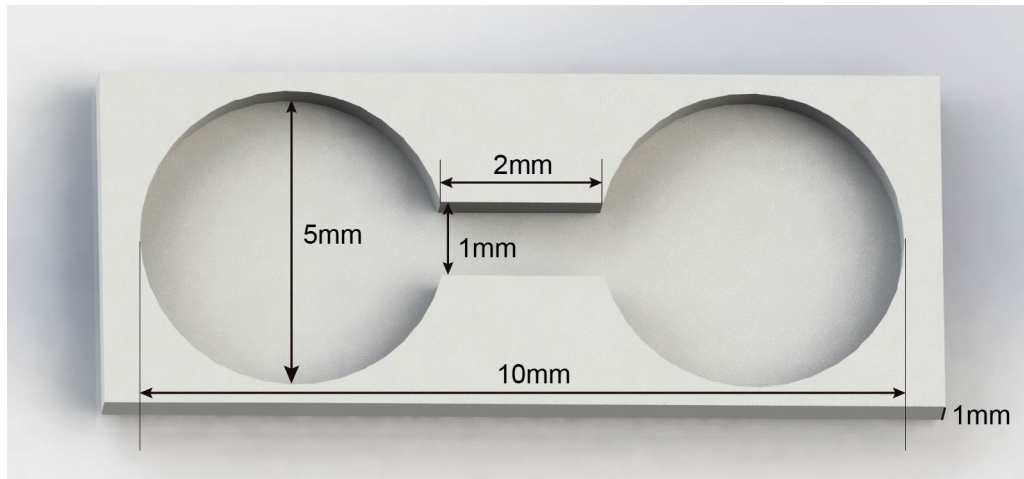


**Figure S12. Schematic of the microchannel phantom for targeted cancer cell elimination.**

Detailed information the microfluidic chip employed for the elimination tests described in the manuscript.



**Figure S13. Microchannel for targeted cancer cell elimination.** The PDMS channel and cleaned glass substrates were treated by oxygen plasma and were bonded together through siloxane bonds. Taking the pure cancer cell medium DMEM to fill the whole microrod channel. After that, a small amount of cancer cells was injected into the left chamber of the microchannel. The channel and the right chamber were kept as blank. Finally, using a pipette to place the magnetic ECM-mimicking microrobot into the left chamber of the microchannel, covering it with a glass.

**Video S1.** Magnetic control of the magnetic ECM-mimicking microrobot following a rectangular trajectory.

**Video S2.** Locomotion of the magnetic ECM-mimicking microrobot in the cell medium.

**Video S3.** Cancer cell capturing by the magnetic ECM-mimicking microrobot in cell culture medium.

**Video S4.** Capturing stability test by spinning the cell-carried microrobot under a magnetic field with high frequency.

**Video S5.** Cancer cell capturing by the magnetic ECM-mimicking microrobot in the blood.

**Video S6.** Cancer cells eliminating by the ECM-mimicking microrobot in a microfluidic chip.